Analyst

PAPER

View Article Online
View Journal | View Issue

Cite this: *Analyst*, 2014, **139**, 5843

AF4/MALS/QELS/DRI characterization of regular star polymers and their "span analogs"

Leena Pitkänen and André M. Striegel*

Received 19th June 2014
Accepted 18th August 2014

DOI: 10.1039/c4an01105h

www.rsc.org/analyst

Asymmetric flow field-flow fractionation (AF4) coupled with multi-angle static and quasi-elastic light scattering and differential refractive index detectors, was employed for the separation and characterization of regular star-shaped polystyrenes and their linear and span analogs in tetrahydrofuran. Stars with different arm lengths were separated from each other by employing a binary slope cross-flow gradient. Cross-flow optimization enabled fast separation of polystyrenes in two- and three-component blends. Macromolecular parameters were obtained by using light-scattering and refractive index detection, and properties of polystyrenes with different molecular architectures were compared. To our knowledge, this is the first report on the separation of star polymers by AF4. Novel characterization approaches for stars are important from both applied and fundamental standpoints, as these macromolecules are valued for their tribological, drug delivery, catalytic and coating capabilities, and also serve as model compounds for the structured study of long-chain branching and its effects in polymers.

Introduction

Field-flow fractionation (FFF) is a family of elution-based techniques that can be employed for the separation of polymers, particles and colloids over a wide size range, from single-digit nanometers to tens of micrometers.[1–3] In FFF, the separation occurs in a thin channel under laminar flow conditions with a pseudo-parabolic flow velocity profile along the thin axis. Polymers/particles of different size arrange themselves within the channel in different mean layer thicknesses from the accumulation wall and, thus, elute from the channel with different velocities. The retention of analytes is influenced by an external field, applied perpendicularly to the separation axis.[4,5] FFF techniques are divided into sub-techniques based on this external field, a flow field being the most universally applicable and, hence, the most commonly used.[6] Because FFF is considered a gentle separation technique, compared to packed column chromatographic techniques, flow field-flow fractionation, particularly asymmetric flow field-flow fractionation (AF4), has become a widely used separation method for many, often large-sized, water-soluble (bio)polymers and particles.[4,7] However, only a few AF4 studies have been performed by employing organic solvents as carrier fluids,[8–11] mainly due to a lack of membrane materials and channel designs compatible with these solvents. Additionally, the use of high-viscosity solvents, such as dimethylsulfoxide, may cause problems when used with currently available AF4 instrumentation because of the disturbance of cross-flow through the membrane caused by the high viscosity of the solvent. Sample dilution, which is more pronounced in AF4 compared to chromatographic techniques, might also restrict the use of certain solvents when the polymer-solvent combination has a low specific refractive index increment ($\partial n/\partial c$).

Separation in AF4 is based on differences between translational diffusion coefficients (D_T) of different analytes. Retention time is inversely proportional to D_T so that, when the external flow field (the so-called "cross-flow") is constant, AF4 functions simultaneously as both a separation and a size characterization method. Because small molecules have larger D_T than large molecules, small molecules diffuse closer to the channel center where the flow velocity in the parabolic flow profile is the highest and, thus, elute before large molecules. Using the well-known Stokes–Einstein relation, these D_T can be converted into a size parameter, namely the hydrodynamic (Stokes) radius R_H of the analyte, *via* eqn (1):

$$R_H \equiv \frac{k_B T}{6\pi\eta_0 D_T} \quad (1)$$

where k_B is Boltzmann's constant, T is the absolute temperature, and η_0 is the solvent viscosity at the experimental temperature. It should be noted that, except for homogeneous hard spheres, this R_H corresponds to a hard sphere equivalent radius, *i.e.*, to the radius of a homogeneous hard sphere with the same D_T as the analyte.[12] Deriving reliable size data from first principles using the FFF retention theory, however, is generally fraught with error, as it requires extremely accurate

National Institute of Standards and Technology, Chemical Sciences Division, 100 Bureau Drive, MS 8392, Gaithersburg, MD 20899, USA. E-mail: andre.striegel@nist.gov; Fax: +1-301-977-0685

determination of various channel and operational parameters. These types of calculations are adversely affected by interactions between the sample and the AF4 membrane and, in the case of channel overloading, by mutual interference effects which prevent individual bands from reaching equilibrium within the channel during the timeframe of the separation.

The above challenges to the calculation of analyte size can be circumvented by the use of on-line light scattering detection techniques such as multi-angle static light scattering (MALS, which measures the radius of gyration, R_G) and/or quasi-elastic light scattering (QELS, also known as dynamic light scattering, which determines R_H). Adding a concentration-sensitive detector, such as differential refractometer (DRI), to the MALS/QELS detector train allows for calculation of the averages, dispersity, and distribution of both R_G and R_H, as well as the molar mass of the sample, and of the size and molar mass of each fraction eluting from the AF4 channel. This type of triple-detector set-up (*i.e.*, AF4/MALS/QELS/DRI), has the added advantage of allowing the use of multi-step cross-flow gradients (*i.e.*, gradients with multiple slopes) in a single AF4 run. While it is possible to calculate R_H from first principles in AF4, when employing decaying cross-flows these calculations are neither straightforward nor have they been found to be particularly accurate, especially when employing very steep cross-flow gradients.[13,14]

Here, we have employed AF4 with multiple detectors to characterize star polymers. Star polymers are branched polymers where a single branch point acts as a core to which multiple linear chains are attached as arms (Scheme 1). Stars can be further categorized based on the structure of the attached arms. Recent advances in the field of polymerization techniques (such as radical and emulsion polymerization) have enabled the synthesis of complex star polymer architectures. In regular star polymers, all attached arms are chemically identical and of the same degree of polymerization, whereas in miktoarm star polymers at least two species of arms with varying chemical compositions and/or arm lengths are present.[15,16] Interest in regular star polymers stems from the fact that their rheological and dilute solution properties greatly differ from those of linear analogs with the same molar mass and monomeric repeat units as the stars. Star polymers represent a model for soft "hybrid" spheres, as they have structural features of both linear polymers and colloids.[17,18] Star polymers have found a wide range of applications, from coatings and adhesives to drug delivery, catalysis and semiconductor technologies, among others.[16,19,20] The continued development of new, functional star molecules generates a need for the evaluation of applicability of analytical techniques for the accurate characterization of these potentially complex, branched macromolecules.

As part of the characterization described here, we have compared several regular eight-arm and three-arm polystyrene (PS) stars both to each other as well as to their linear and span analogs. A linear analog is a linear PS of approximately the same molar mass as the star, whereas a span analog is a PS with a molar mass approximating that of two arms of a particular star, as the combination of two arms of a star is commonly referred to as the "span" of the star (Scheme 1). Using AF4/MALS/QELS/DRI, we were able to isolate from each other molar mass and architectural effects such as arm number and arm length, to characterize not only the solution behavior of the analytes but also absolute, solvent/temperature-independent properties of the various stars.

Additional aspects of this study were the investigation of the effects of cross-flow gradients and analyte solution concentration on the separation, fractographic resolution and sample recovery. As we shall see, performing AF4 analyses in an organic solvent allowed for separation of star and linear PSs, and multiple-detection allowed for determination of molar mass and size without system calibration. The use of cross-flow gradients has enabled the separation of samples which differed from each other by more than one order of magnitude in molar mass, but also of samples which differed in size by only ≈2 nm.

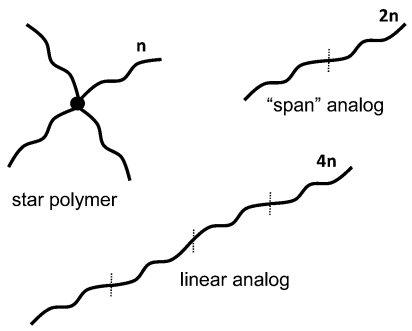

Scheme 1 Schematic presentation of a star polymer and its "span" and linear analogs. The degree of polymerization (DP) of one star arm is represented by *n*. Thus, the DP of a "span" analog is always 2*n*, but the DP of a linear analog is the number of arms in the star multiplied by *n*. Note that *n* represents only DP (directly proportional to molar mass) and not the actual size or dilute solution conformation of a polymer.

Experimental

Samples

Linear PS samples with reported weight-average molar mass M_w of 19 760 g mol^{-1} and 49 170 g mol^{-1} were purchased from Agilent/Polymer Laboratories (Amherst, MA), and with M_w of 243 000 g mol^{-1} from PSS Polymer Standards Service (Mainz, Germany). Eight-arm star PS with M_w of 94 800 g mol^{-1} (number-average molar mass M_n of each arm 9800 g mol^{-1}) and 247 000 g mol^{-1} (M_n of each arm 25 300 g mol^{-1}) were from PSS Polymer Standards Service. High-molar mass eight-arm star PS (M_w of 1 229 000 g mol^{-1}, M_n of each arm 137 000 g mol^{-1}) was purchased from Polymer Source, Inc (Dorval, Canada). Three-arm star PS (M_w 300 000 g mol^{-1}) with equal arm lengths was from Polysciences, Inc (Warrington, PA). Sample nomenclature was adopted from Striegel,[21] where PS-L refers to linear PS and PS-StX to star polymer with *X* number of arms, followed by M_w (reported by the manufacturer) in kg mol^{-1} for linear samples, and by $M_{n,\,star}/M_{w,\,total}$ in kg mol^{-1} for star samples (*e.g.*, PS-L 20

or PS-St8 9.8/95). Tetrahydrofuran (THF) was from Avantor Performance Materials (Center Valley, PA).

AF4/MALS/QELS/DRI

The multi-detector AF4 instrument consisted of an Agilent 1260 isocratic HPLC pump (Agilent Technologies, Santa Clara, CA), an autosampler (Agilent 1260), an Eclipse DualTec FFF control module (Wyatt Technology Co., Santa Barbara, CA), a DRI detector (T-rEX, Wyatt Technology Co.), a MALS photometer (DAWN HELEOS-II, Wyatt Technology Co., 16 measurement angles, with nominal values ranging from 28° to 147°), and a QELS detector (Wyatt Technology Co.) in the same housing as the MALS unit. QELS measurements were performed at a nominal angle of 108° relative to the incident laser beam. A 0.22 μm inline Teflon® filter was placed after the pump and before the injector.

The AF4 separation occurred in an open channel consisting of a bottom plate with a porous frit and an upper, non-permeable plate (giving the prefix "asymmetric" to the technique's name, in contrast to a symmetrical channel, in which both plates are permeable). The frit was covered with a regenerated cellulose ultra-filtration membrane with a nominal 5 kDa cut-off. The channel thickness was defined by placing a 490 μm Mylar® spacer between the membrane and the upper plate. The spacer had a trapezoidal shape, with tip-to-tip length of 173 mm and cross-sectional width at focusing zone of 22 mm. Due to the compressibility of the membrane, the actual channel thickness is ≈10% lower than the spacer thickness. In principle, separation can be divided into two stages: the injection/focusing step and the elution step. Here, the injection/focusing time was 3 min and the focusing flow was 1.5 mL min^{-1}. In the Eclipse DualTec, during focusing all the flow entering into the channel goes through the membrane to waste, as cross-flow. The detector flow, which by-passes the channel in the injection/focusing step, was kept constant throughout the analyses. The DRI signal of a THF solvent blank was subtracted from the DRI signals of all sample runs.

Normalization of the MALS detector (vacuum wavelength of incident light, $\lambda_0 = 664.5$ nm), inter-detector alignment, and inter-detector band broadening correction were performed using a narrow-dispersity ($M_w/M_n \leq 1.06$) PS standard with M_w of 30 000 g mol^{-1} (Pressure Chemical Co.). MALS, QELS, and DRI data were collected and processed using ASTRA software (Wyatt Technology Co., version 6.1.1.17). Zimm's first-order formalism was employed for MALS data fitting to determine molar mass and radius R_G of each eluting fraction. The polymer samples were dissolved in stabilized THF prior to AF4 analyses, at a concentration of 1 mg mL^{-1}, 2 mg mL^{-1}, or 5 mg mL^{-1}. The AF4 analyses of blends were performed in triplicate from two separate sample dissolutions, at a total polymer concentration of 1 mg mL^{-1}. Analyses of individual samples were performed at a concentration of 5 mg mL^{-1} (2 mg mL^{-1} for PS-St8 137/1229), in triplicate from one sample dissolution. The concentrations employed for the analysis of individual samples are, however, far below the critical overlap concentration c^* of the largest sized molecules present in the samples, with c^* calculated as per eqn (2):

$$c^* = \frac{M_w}{\left(\frac{4\pi}{3}\right) N_A R_G{}^3} \quad (2)$$

where N_A is Avogadro's number.[18] The c^* values of the largest sized molecules of the sample were 8.5 mg mL^{-1} for PS-L 243 and 9.1 mg mL^{-1} for PS-St 8 137/1229. For a given architecture, c^* values for samples with lower (nominal) molar masses are expected to be lower than the values just given. The injection volume for all analyses was 50 μL. The AF4 channel was maintained at room temperature and the detectors at 25 °C.

Specific refractive index increment ($\partial n/\partial c$) determination

A linear PS sample (M_w 200 000 g mol^{-1}, $M_w/M_n = 1.06$, Pressure Chemical Co., Pittsburg, PA) was used for $\partial n/\partial c$ determination. The sample was dissolved in THF at five concentrations ranging from 1 mg mL^{-1} to 5 mg mL^{-1}. Each dilution was injected directly into the differential refractometer cell (same T-rEX detector as employed in the on-line experiment; vacuum wavelength of light $\lambda_0 = 658$ nm, within 7 nm of the λ_0 of the MALS/QELS photometer) using a Razel model A-99EJ syringe pump at a flow rate of 0.1 mL min^{-1}, at 25 °C. The samples and neat THF were filtered gently before measurement using 0.22 μm Teflon® syringe filters (VWR, Radnor, PA). ASTRA software (Wyatt Technology Co., version 6.1.1.17) was used for data collection and processing. The $\partial n/\partial c$, obtained from the slope of a plot of concentration *versus* differential refractive index, for PS in THF ($\lambda_0 = 658$ nm, 25 °C) was 0.196 mL $g^{-1} \pm 0.002$ mL g^{-1}. The $\partial n/\partial c$ plot, with associated concentration data for each dilute solution analyzed, can be found in the ESI of ref. 22.

Given that $M_{arm} >> M_{core}$ for the star polymers, and that the arms are non-oligomeric in length (*i.e.*, end group effects on $\partial n/\partial c$ are expected to be insignificant), the $\partial n/\partial c$ of the stars can reasonably be considered to be equal to that of linear PS at identical experimental conditions, especially as this has been the case in other solvent systems.[21]

Results and discussion

Star and linear PSs were characterized by multi-detector AF4 individually as well as in the following blends: ternary blend of linear PSs (PS-L 20 + PS-L 50 + PS-L 243), ternary blend of star PSs (PS-St8 9.8/95 + PS-St8 25/247 + PS-St8 137/1229), binary blend of eight-arm star PS and linear PS (PS-St8 25/247 + PS-L 243) samples with similar molar masses to each other and, finally, a blend of two stars with different architecture but the same molar mass as each other (PS-St8 25/247 + PS-St3 85/300). The effect of concentration on the AF4 separation, the importance and challenges of reporting sample recovery, and the optimization of cross-flow conditions will be addressed in upcoming sections. First, however, we characterize and contrast the analytes with respect to molar mass, size and structure.

Molar mass, size, and architectural features of star PSs

Molar mass, R_G, and R_H are plotted across the DRI peaks in the fractogram overlays of linear (Fig. 1a) and eight-arm star

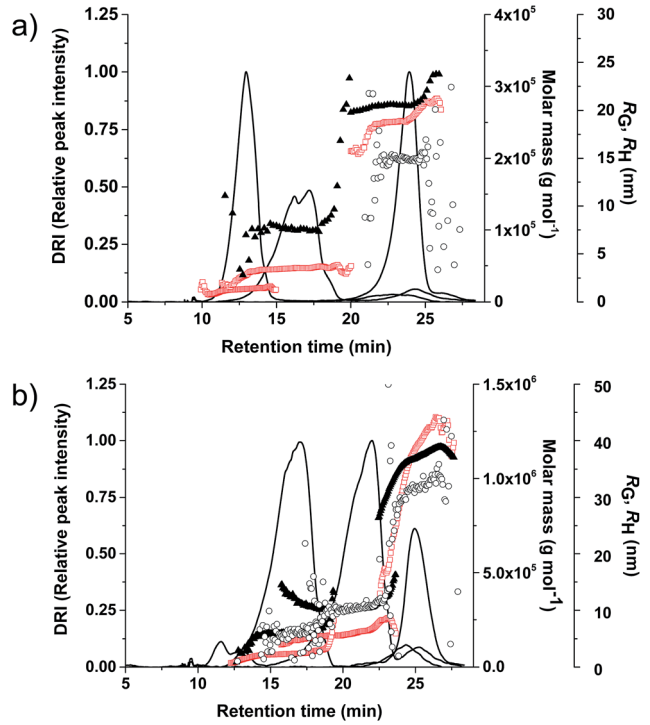

Fig. 1 Normalized overlay of fractograms (DRI response, solid black lines) for individual (a) linear PS samples and (b) star PS samples. A concentration of 5 mg mL^{-1} (except 2 mg mL^{-1} for PS-St8 137/1229) was used in order to obtain quantifiable QELS data for the determination of R_H. Molar mass across the peaks is presented as open red squares, R_G as black filled triangles, and R_H as open black circles. The AF4 analysis conditions correspond to the ones presented in Fig. 2b and c.

(Fig. 1b) PSs. The molar mass averages, molar mass dispersity (M_w/M_n), *z*-average sizes (R_G, R_H), and the dimensionless size parameter ρ ($\equiv R_{G,z}/R_{H,z}$) for both linear and star PSs are given in Table 1. In this table, the R_H values of PS-L 20 and PS-L 50 were calculated using the relationship between R_H and M_w as recently determined by Wernert *et al.*,[23] because quantifiable QELS data would have required substantially higher solution concentration than even the highest concentration employed in these studies. As seen in Table 1, the calculated R_H of PS-L 20 and PS-L 50 were 4 nm and 6 nm, respectively. The fractogram for these polymers (in a ternary blend which also contained PS-L 243) is shown in Fig. 2a and it demonstrates the ability of AF4 to separate analytes which differ from each other only minimally in size.

In general, when characterizing branched polymers (*e.g.*, stars), their properties are compared to those of linear polymers with the same chemical composition and molar mass.[24–29] Here, however, we have focused on comparing the properties of star PSs to linear PSs having a molar mass equal to the M_{span} of the star, with $M_{span} = 2 \times M_{arm}$. The original intent was that (for stars with low arm number) a linear PS having the M_{span} of a star would serve as a linear analog ("span analog") of a size or hydrodynamic volume similar to that of the star. The parameter M_{span} was previously shown to govern the mechanochemical degradation of low-arm number ($f \leq 8$) stars in dilute solution,[21] and has also been proposed as a mean molecular dimension in the interpretation of SEC data.[30] Experimentally, however, we have found the size, be it R_H or R_G, of the eight-arm star PSs to be clearly larger than that of their span analogs. The difference in size also manifests itself as different AF4 elution times for the eight-arm stars and corresponding span analogs in Fig. 2b and c, and can be explained as follows.

The larger radius of a star, compared to that of a span analog, can be explained by the higher chain stiffness of arms in star polymers as compared to the chain stiffness of individual, unattached linear chains. The difference in chain stiffness becomes more pronounced as the number of arms in a star molecule increases. Chain mobility in star arms becomes more limited near the star core due to increase in chain crowding, resulting in deviations from the Gaussian chain behavior. Thus, chains are more stretched out (*i.e.*, larger in size) as arms in star molecules than they are as individual, unattached linear chains. This stretching-out effect is less prevalent in the peripheral regions of star molecules, and becomes less significant as the arm length increases; two repeat units, each located on the periphery of consecutive star arms, are farther away from each other, and can thus influence each other less, than when located on the same arms in positions near the star core.[24,31] The consequence of the arm number in stars causing non-Gaussian chain behavior can be observed in the size data when we compare the R_H of three-arm and eight-arm star PSs to the R_H values obtained for their span analogs. Because we were unable

Table 1 Molar mass averages, molar mass dispersity (M_w/M_n), radius of gyration (R_G), hydrodynamic radius (R_H), and R_G/R_H for linear and star PSs[a]

	M_n (g mol^{-1})	M_w (g mol^{-1})	M_z (g mol^{-1})	M_w/M_n	R_G[b] (nm)	R_H[b] (nm)	$R_G/R_H \equiv \rho$[c]
PS-L 20	18 200 ± 100	18 300 ± 100	18 400 ± 100	1.00 ± 0.01	nd[d]	3.9[e]	nd
PS-L 50	47 300 ± 100	47 400 ± 100	47 800 ± 200	1.00 ± 0.00	8.0	6.3[e]	1.3
PS-L 243	255 600 ± 800	255 800 ± 900	256 100 ± 900	1.00 ± 0.01	21	15	1.4
PS-St8 9.8/95	68 700 ± 1000	70 400 ± 1000	71 800 ± 1200	1.02 ± 0.02	6.3	5.9	1.1
PS-St8 25/247	184 600 ± 2100	188 200 ± 2200	191 900 ± 2500	1.02 ± 0.02	10	11	1.0
PS-St8 137/1229	1 089 000 ± 31 000	1 131 000 ± 23 000	1 161 000 ± 27 000	1.04 ± 0.04	37	32	1.2
PS-St3 85/300	259 000 ± 500	262 000 ± 200	265 100 ± 100	1.01 ± 0.00	20	15	1.4

[a] Data obtained for samples analyzed individually with the concentration 5 mg mL^{-1} (2 mg mL^{-1} for PS-St8 137/1229). Uncertainties reflect one standard deviation, based on triplicate injections, as specified in Experimental. [b] *z*-average values for both radii; in all cases, standard deviations < ± 1 nm. [c] Based on *z*-averages of both radii, standard deviations of all ρ values < ± 0.1. [d] nd = not determined. [e] Estimated using the following power-law relation for linear PSs:[23] $R_H = (0.024 \pm 0.002)(M_w)^{0.518\pm0.005}$.

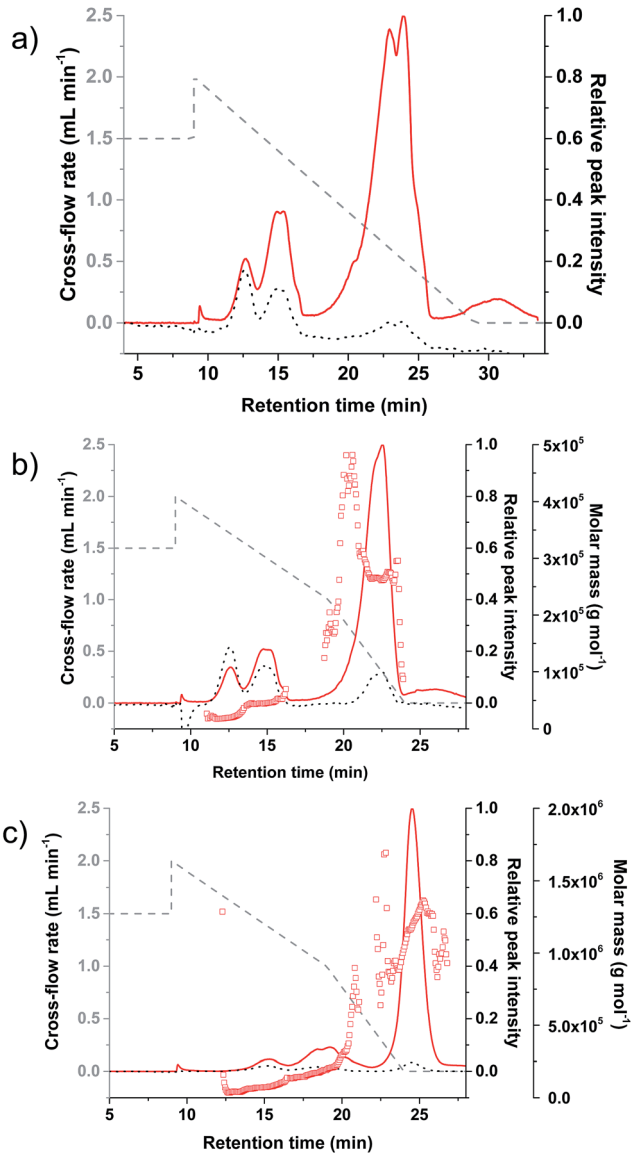

Fig. 2 AF4 fractograms (solid red line represents normalized static light-scattering signal at 90° and dotted black line represents normalized DRI signal) for (a) and (b) blend of linear PSs PS-L 20, PS-L 50 and PS-L 243, and (c) blend of star PSs PS-St8 9.8/95, PS-St8 25/247 and PS-St8 137/1229, all analyzed using a linearly decaying cross-flow gradient (dashed gray line) with an initial cross-flow of 2 mL min^{-1}. In (a) the slope of the gradient is 0.1 and in (b) and (c) an additional gradient with a slope of 0.2 is included starting at 19 minutes. In all analyses, elution starts at 9 minutes. Molar mass across the peaks is presented as open red squares in (b) and (c).

to obtain a narrow dispersity PS with a molar mass of 170 000 g mol^{-1}, which is the molar mass of the span in PS-St3 85/300, the R_H of this span analog was calculated by employing the recently published relation[23] $R_H = (0.024 \pm 0.002)(M_w)^{0.518\pm0.005}$, derived from data for PS in THF at 25 °C, *i.e.*, under the same experimental conditions as in our study. This relation has provided an R_H of 12 nm for the span analog of the three-arm star. The size (R_H) of the three-arm star PS is close to the value of its span analog (15 nm *versus* 12 nm) whereas, for all eight-arm stars, the star dimensions are higher in comparison to their span analogs due to the previously described stretching-out effect.

In addition to contrasting each eight-arm star to its respective span analog, we were also able to compare PS-St8 25/247 and PS-St3 85/300 (both of which have similar molar masses to each other), to their linear analog (not to be confused with span analog) PS-L 243. While the size of the eight-arm star PS was smaller than that of its linear analog, the size of the three-arm star and the linear analog were virtually identical to one another. The reason behind these dissimilar and seemingly counterintuitive (at least when taken together) observations is that, in the case of eight-arm star, the difference between its span molar mass ($\approx$50 000 g mol^{-1}) and the molar mass of its linear analog is too great to overcome polymer expanding effects (as discussed in the previous paragraph) due to chain crowding in the vicinity of the star core. In the three-arm star these chain expanding effects are smaller than in the eight-arm star, as a result of less crowding due to a smaller number of arms. However, the relative difference between M_{span} and molar mass of the linear analog is substantially smaller for the three-arm star ($M_{linear\ analog}/M_{span\ analog} \approx 1.4$) as compared to the eight-arm star ($M_{linear\ analog}/M_{span\ analog} \approx 5$). Hence, these two effects, chain expansion and molar mass ratio of linear analog to span analog, compensate each other almost completely in the three-arm star studied, leading the latter to have a similar size in solution to its linear analog.

We note also that the comparison of the mean-square radii of star polymers with their linear counterparts of the same molar mass, $(R_G)^2_{star}/(R_G)^2_{linear}$, has been studied extensively in both θ-state and thermodynamically good solvent/temperature conditions (as has been done here, comparisons are understood to be among linear and star polymers composed of the same monomeric repeat units as each other).[25] This ratio is known to decrease as a function of increasing arm number as, with increasing arm number, the same molar mass must now be distributed among a larger number of arms, resulting in shorter arms and, consequently, in a smaller dilute solution chain dimension.[17] The ratio of the mean-square radii for star PS PS-St8 25/247 and its linear counterpart PS-L 243 was 0.30, while the same ratio for PS-St3 85/300 and PS-L 243 was 0.72 (using the R_G value of the elution slice with a molar mass of $\approx$ 220 000 g mol^{-1}). Both these values are well in accordance with results from the literature, which show that, at good solvent/temperature conditions, the ratio of the mean-square radii of three-arm star polymers to their linear counterparts ranges between 0.72 and 0.78, while the measured ratios for eight-arm stars range from 0.34 to 0.35.[32]

As mentioned earlier in this section, the multi-detector AF4 approach allowed us to determine the two size parameters R_G and R_H, as well as their ratio with respect to each other. This ratio is given by the dimensionless size parameter ρ, which is meant to describe the macromolecular architecture in a molar-mass-independent fashion. Theoretical values of ρ have been derived, for various architectures, at both θ and good solvent/temperature conditions.[24] For example, the theoretical ρ value for homogeneous hard spheres is $\approx$ 0.77, with increasingly higher ρ values generally corresponding to increasingly less

compact structures in solution. Here, we have observed (Table 1) that the ρ values of the linear PSs studied are quite similar to each other, regardless of large differences in molar mass, a statement which also holds true for the eight-arm star polymers examined. Moreover, the ρ values of the eight-arm stars are lower than those of the linear polymers, reflecting the more compact nature of the stars.

As seen in Table 1, the ρ values of the 3-arm star and its linear analog are identical to one another. This is due to the fact that a linear polymer can be considered as a star with two arms. The addition of only one arm to this structure does not appreciably alter the solution compactness of the macromolecular arrangement. This structural similarity results in the three-arm star examined here having a ρ value immeasurably different from that of the linear PSs examined and, thus, also higher than the ρ values of the eight-arm stars.

Optimization of AF4 cross-flow gradients

Linear PS blend and eight-arm star PS blend. As mentioned in Introduction, optimizing the cross-flow in AF4 is important with regard to resolution and sample recovery. Here, a blend of the three linear PSs (PS-L 20 + PS-L 50 + PS-L 243) was used for cross-flow optimization. The cross-flow rate can be constant during elution or it can decrease as a function of time, most commonly either in a linear or exponential fashion. Based on previous AF4 studies of narrow dispersity PSs, a decaying cross-flow gradient was chosen over a constant cross-flow.[8,10] The linearly decaying gradient with an initial cross-flow of 2 mL min^{-1}, decreasing to 0 mL min^{-1} over the course of 20 min (gradient slope of 0.1 mL min^{-2}; because the slope is used here only to describe the steepness of a gradient, the units are omitted hereafter), separated the three linear PSs with different molar masses from each other within the elution gradient in the order of increasing molar mass (this order is expected based on the normal retention mode theory of AF4[33]) (Fig. 2a). In this case, however, the light scattering peak shape of PS-L 243 was both broad and split into two at the peak apex. To overcome these issues, an additional gradient, with a higher slope of 0.2, was added to the elution step at 19 min. In this way, the two lower-molar mass linear PSs (PS-L 20 and PS-L 50) were separated from each other using the gradient with a slope of 0.1, as in Fig. 2a, while PS-L 243 was separated from PS-L 50 using the 0.2 gradient. The latter gradient has also served to improve the peak shape of PS-L 243 which, as can be seen in Fig. 2b, is both narrower and no longer artificially split at the apex, as expected for a narrow dispersity PS. The decrease in peak width of PS-L 243, when using the gradient with two slopes, can be explained by the steeper slope of the additional gradient (*i.e.*, cross-flow decreases faster) which allows the peak to elute faster. The improvement of the peak shape might be due to higher signal-to-noise ratio (S/N) of the PS-L 243 peak when employing the additional slope in the separation gradient, as compared to the S/N when the gradient had only one slope of 0.1. The same gradient with two slopes was also used for separating a blend of three eight-arm star PSs (PS-St8 9.8/95 + PS-St8 25/247 + PS-St8 137/1229), as shown in Fig. 2c.

Blend of PSs of the same molar mass but different architecture. The cross-flow gradient that was developed for the separation of blends of linear PSs, and of blends of eight-arm star PSs, was then evaluated for separating a blend of an eight-arm star PS and a linear PS with nearly equal molar masses to each other (PS-St8 25/247 + PS-L 243). As shown in Fig. 3, most of the injected polymer elutes during the second section of the gradient (this gradient is represented as a dashed red line in Fig. 3; the fractogram corresponding to this gradient is represented as a red line with triangles in the same figure), and two peaks corresponding to the two components in the blend can be observed in the fractogram. Our next effort was aimed at improving the resolution of this separation. Because this binary blend did not contain a low-molar mass analyte (as was the case in both three-component blends described in the previous section), we were able to decrease the cross-flow during the initial stage of the separation from 2 mL min^{-1} to 1.5 mL min^{-1} (solid black line in Fig. 3). Lowering the initial cross-flow decreased the retention times for both analytes (black line with circles). The slope in the first section of this gradient (from 1.5 mL min^{-1} at 9 min to 0.7 mL min^{-1} at 19 min) was 0.08, nearly identical to the slope of 0.1 employed in the initial portion of the gradient used for separating the three-component blends discussed previously. Star PS PS-St8 25/247 which, as in Table 1, has a smaller hydrodynamic radius than its linear analog PS-L 243, elutes during the first section of the gradient. After elution of this star, the cross-flow was decreased from 0.7 mL min^{-1} to 0 mL min^{-1} over the course of 5 min (slope of 0.14). This combination of gradients resulted in the improved separation of these two polymers (Fig. 3 and 4a), as compared to the separation obtained when employing the gradient designed

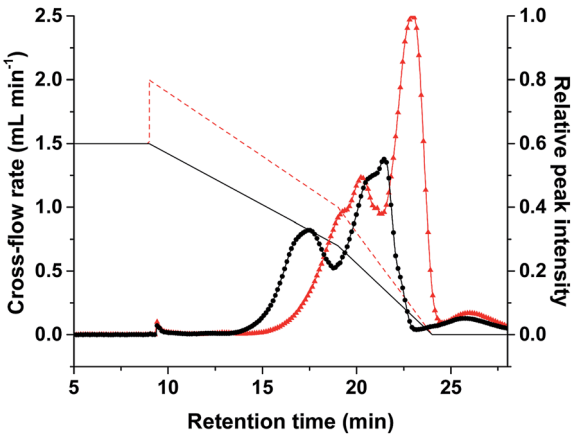

Fig. 3 Effect of cross-flow on the separation of PS-St8 25/247 (first peak) and PS-L 243 (second peak). The gradient employed in this separation (solid black line) has a lower (1.5 mL min^{-1}) initial cross-flow than did the gradient employed in the separation shown in Fig. 2b and c (the latter gradient is shown, for comparison, as a dashed red line in the current figure). The relative peak intensity (static light-scattering signal of 90° photodiode) is presented in the fractogram overlay (red line with triangles for gradient with an initial cross-flow of 2 mL min^{-1} and black line with circles for gradient with an initial cross-flow of 1.5 mL min^{-1}). Elution starts at 9 minutes.

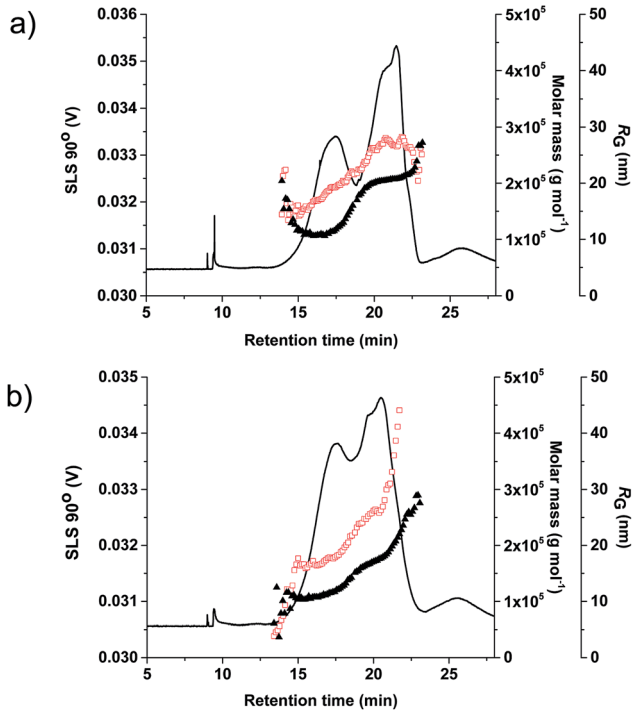

Fig. 4 Fractograms showing static light-scattering signal (SLS 90°, solid black line), molar mass (open red squares), and radius of gyration (R_G, black filled triangles) for binary blends of (a) PS-St8 25/247 (first peak in the fractogram) and PS-L 243 and (b) PS-St8 25/247 (first peak in the fractogram) and PS-St3 85/300. Cross-flow gradient used for the separation is presented in Fig. 3 as a black solid line. Elution starts at 9 minutes.

for binary blends of different molar mass PSs of the same architecture (linear or eight-arm stars).

The cross-flow gradient designed for the separation of PS-St8 25/247 and PS-L 243 was also used to separate of a blend of an eight-arm star and a three-arm star PS with similar molar masses, namely PS-St8 25/247 and PS-St3 85/300. Two peaks can be observed in the fractogram in Fig. 4b, although the peak overlap is larger in this case than it was in the separation of the eight-arm star and linear PS with identical molar mass (Fig. 3). This overlap of peaks is expected, because the size difference between PS-St8 25/247 and PS-St3 85/300 is known to be smaller than the size difference between PS-St8 25/247 and PS-L 243.[21]

Analyte concentration effects in AF4

The total sample concentration of all analytes in blends was 1 mg mL^{-1}. For an injection volume of 50 μL, the total sample amount injected into the channel was 50 μg, 16.7 μg of each analyte in the ternary blends (Fig. 1), and 25 μg per analyte in the binary blends (Fig. 3 and 4). These amounts were sufficient for MALS and DRI detection (*S*/*N* for each analyte ranged from 30 to 700) and for the determination of both molar mass and R_G (Fig. 2 and 4). To obtain quantifiable QELS data, however, each polymer was analyzed individually at a concentration of 5 mg mL^{-1} (2 mg mL^{-1} for the highest-molar mass star sample, PS-St8 137/1229). Even when using a concentration of 5 mg mL^{-1}, the QELS *S*/*N* for PS-L 20 and PS-L 50 were too low to allow for an accurate determination of the R_H of these analytes (an approximate 10-fold increase in *S*/*N* would have been needed to determine their R_H). As described earlier, the R_H of these analytes was instead calculated by employing the R_H *versus* molar mass relation given by Wernert *et al.*[23]

The overlay of fractograms for individual linear and star PSs, each at a concentration of 5 mg mL^{-1}, is presented in Fig. 1. When these fractograms are compared with those of the same samples analyzed at lower concentrations (blends of either linear or star PSs at a total sample concentration of 1 mg mL^{-1}, Fig. 2), it can be observed that, as the analyte concentration increases, so does the peak breadth. In AF4 (as in most separation methods), band broadening is usually more severe and the most noticeable in the case of narrow molar mass dispersity samples. Because in AF4 the analytes form layers in the flow stream according to their size, if a sample is narrowly disperse then the transversal thickness of the analyte layers in the flow increases with increasing concentration. This effect is more pronounced for high molar mass (large-sized) molecules than it is for low molar mass (small-sized) ones. When the sample is polydisperse (or broadly disperse), however, higher concentrations can be employed without noticeable peak broadening, due to sample components of different diffusion coefficients distributing to different flow layers (*i.e.*, due to the distribution of diffusion coefficients that exists in a disperse sample). A natural consequence of this channel overloading phenomenon (especially in regards to narrow dispersity analytes) is that, for multicomponent samples, as the breadth of the individual bands increases, the resolution of the separation deteriorates. The adverse effect of increasing concentration on band broadening can be observed in Fig. 1 as overlapping peaks of the two lower molar mass samples with both linear and star shape structures (PS-L 20 *versus* PS-L 50 and PS-St8 9.8/95 *versus* PS-St8 25/247).

Although channel overloading is regarded as a fundamental problem in AF4, it can be considered acceptable for individual narrow dispersity samples when size and molar mass data are obtained using MALS, QELS and DRI detection, because molar mass, R_G and R_H are actually measured by these detectors (*i.e.*, they are not derived from retention time and calibration curves or calculated using the FFF theory). Comparison of molar mass and R_G data from blends (where the amount injected was 16.7 μg or 25 μg, as per Fig. 2 or 4, respectively) with data from individual samples injected in amounts ranging from 100 μg to 250 μg (Fig. 1) shows that the determination of both molar mass and size is not influenced by concentration in the present experiments. Thus, overloading the channel to obtain R_H data in addition to R_G data for each individual PS sample is acceptable in the present case.

Recovery analysis

The quantitation of sample recovery in AF4 analyses is important for the purposes of both precision and accuracy. Ideally, 100% of the sample should be recovered from the AF4 channel (as it should be from any separation), with the second most

desirable scenario being the sample loss that is unbiased with respect to molar mass, size, or chemical composition. The recovery analyses were based on the areas of the DRI peaks (the differential refractometer being a concentration-sensitive detector) of individually analyzed samples, at a concentration of either 2 mg mL^{-1} or 5 mg mL^{-1}. The sample recovery for linear PS samples was 78% ± 1% and for star PS samples it was 79% ± 3%, in general agreement with previously reported recovery values for PSs in AF4.[10] In all cases, sample recovery was found to be independent of analyte molar mass, size, and architecture.

Contrary to the case of column chromatography, AF4 is not a closed system due to the permeable frit in the channel. Because of the latter, 100% recoveries are rarely achieved in AF4. In earlier AF4 studies on the separation of broadly distributed PS it was observed that, although the transport of low-molar mass molecules through the membrane clearly dominates over that of higher-molar mass molecules, some molar mass independent transport of molecules through the membrane occurs as well.[10] Molecules with even higher molar mass than the nominal cut-off value of the membrane have been reported to pass through the latter during AF4 analysis.[10] Additionally, molecule-membrane interactions may also contribute to reduced sample recovery. Recoveries, however, are always strongly dependent on the experimental conditions and instrumental set-up used, as well as on the identity of the analyte. Because recovery could already be considered high for AF4 (≈80%) in our initial experiments, additional optimization of analytical conditions with respect to recovery was not considered necessary.

It should be noted that different ways of reporting sample recovery in AF4 can be found in the literature. Some authors prefer to compare the concentration detector peak area for a given AF4 run with the peak area determined without cross-flow for the same analyte. This approach usually gives higher recovery values compared to the recovery calculated directly from the concentration detector response and known $\partial n/\partial c$ (if DRI is the concentration-sensitive detector, as in this study) or molar absorptivity (when a UV spectrophotometer is used to measure concentration), because of the comparatively minor sample loss which occurs in the absence of cross-flow. The third reported procedure to calculate recovery is to replace the channel with tubing or a union and compare the concentration detector area of the separated analyte with the area obtained by running the sample only through the capillary. The various methods employed to calculate sample recovery in AF4 make it difficult to directly compare the recovery values reported in different studies.

Conclusions

We have demonstrated the applicability of AF4 coupled to MALS, QELS, and DRI detection for the separation and characterization of PS star polymers and their linear and span analogs. Although at present the vast majority of AF4 applications are for the analysis of water-soluble (or water-dispersible), relatively broadly disperse, and often biogenic samples, the technique can also be employed for the analysis of synthetic polymers using organic solvents. Through the use of on-line light scattering detection (both MALS and QELS) in conjunction with the AF4 separation, information on size, in the form of different radii (R_G and R_H), could be obtained in a single run without the determination of exact channel parameters. The separation of linear PSs in three-component mixtures, with the R_H of the samples ranging from ≈4 nm to ≈15 nm, was effected. For star PSs, good resolution could be obtained for a blend containing three components with R_H ranging from ≈6 nm to ≈32 nm and separation of linear PSs was achieved even for analytes the R_H of which differed from each other by only 2 nm. As the synthesis and use of star polymers with different chemistries and functionalities continue to proliferate (*e.g.*, in medicine and nanotechnology), multi-detector AF4 has the realized potential to provide selective and quantitative characterization of stars and related architectures (*e.g.*, H-polymers, dendrimers) over a wide molar mass range.

Acknowledgements

The Finnish Cultural Foundation is greatly acknowledged for funding of L.P. through the Foundations' Post Doc Pool. Commercial products are identified to specify adequately the experimental procedure. Such identification does not imply endorsement or recommendation by the National Institute of Standards and Technology, nor does it imply that the materials identified are necessarily the best available for the purpose.

References

1 J. C. Giddings, F. J. F. Yang and M. N. Myers, *Science*, 1976, **193**, 1244–1245.
2 K.-G. Wahlund and J. C. Giddings, *Anal. Chem.*, 1987, **59**, 1332–1339.
3 S. Podzimek, *Encyclopedia of Analytical Chemistry*, 2012, DOI: 10.1002/9780470027318.a9289.
4 S. K. R. Williams and D. Lee, *J. Sep. Sci.*, 2006, **29**, 1720–1732.
5 S. Podzimek, *Light Scattering, size exclusion chromatography and asymmetric flow field flow fractionation*, Wiley, Hoboken, New Jersey, 2011, p. 259.
6 J. C. Giddings, in *Field-flow fractionation handbook*, ed. M. Schimpf, K. Caldwell and J. C. Giddings, Wiley, New York, 2000, pp. 3–30.
7 G. Yohannes, M. Jussila, K. Hartonen and M.-L. Riekkola, *J. Chromatogr. A*, 2011, **1218**, 4104–4116.
8 D. Y. Bang, D. Y. Shin, S. Lee and M. H. Moon, *J. Chromatogr. A*, 2007, **1147**, 200–205.
9 E. P. C. Mes, H. De Jonge, T. Klein, R. R. Welz and D. T. Gillespie, *J. Chromatogr. A*, 2007, **1154**, 319–330.
10 T. Otte, R. Brüll, T. Macko, H. Pasch and T. Klein, *J. Chromatogr. A*, 2010, **1217**, 722–730.
11 T. Otte, H. Pasch, T. Macko, R. Brüll, F. J. Stadler, J. Kaschta, F. Becker and M. Buback, *J. Chromatogr. A*, 2011, **1218**, 4257–4267.
12 M. J. Smith, I. A. Haidar and A. M. Striegel, *Analyst*, 2007, **132**, 455–460.

13 L. Nilsson, M. Leeman, K.-G. Wahlund and B. Bergenståhl, *Biomacromolecules*, 2006, **7**, 2671–2679.
14 L. Nilsson, *Food Hydrocolloids*, 2013, **30**, 1–11.
15 N. H. Aloorkar, A. S. Kulkarni, R. A. Patil and D. J. Ingale, *Int. J. Pharm. Sci. Nanotechnol.*, 2012, **5**, 1675–1684.
16 H. Gao, *Macromol. Rapid Commun.*, 2012, **33**, 722–734.
17 J. Roovers, in *Star and hyperbranched polymers, Plastics Engineering 53*, ed. M. K. Mishra and S. Kobayashi, Marcel Dekker, New York, 1999, pp. 285–341.
18 D. Vlassopoulos, G. Fytas, T. Pakula and J. Roovers, *J. Phys.: Condens. Matter*, 2001, **13**, R855–R876.
19 J. A. Simms, *Prog. Org. Coat.*, 1993, **22**, 367–377.
20 A. Blencowe, J. F. Tan, T. K. Goh and G. G. Qiao, *Polymer*, 2009, **50**, 5–32.
21 A. M. Striegel, *J. Biochem. Biophys. Methods*, 2003, **56**, 117–139.
22 A. M. Striegel, *J. Chromatogr. A*, 2014, **1359**, 147–155.
23 V. Wernert, R. Bouchet and R. Denoyel, *Anal. Chem.*, 2010, **82**, 2668–2679.
24 W. Burchard, *Adv. Polym. Sci.*, 1999, **143**, 113–194.
25 W. H. Stockmayer and M. Fixman, *Ann. N. Y. Acad. Sci.*, 1953, **57**, 334–352.
26 A. M. Striegel, W. W. Yau, J. J. Kirkland and D. D. Bly, *Modern size-exclusion liquid chromatography*, Wiley, Hoboken, New Jersey, 2nd edn, 2009.
27 A. M. Striegel and M. R. Krejsa, *J. Polym. Sci., Part B: Polym. Phys.*, 2000, **38**, 3120–3135.
28 A. M. Striegel, *Polym. Int.*, 2004, **53**, 1806–1812.
29 A. M. Striegel, in *Encyclopedia of Chromatography*, ed. J. Cazes, Taylor & Francis, New York, 3rd edn, 2010, pp. 1417–1420.
30 Y. Wang, I. Teraoka, F. Y. Hansen, G. H. Peters and O. Hassager, *Macromolecules*, 2011, **44**, 403–412.
31 K. Huber, W. Burchard, S. Bantle and L. J. Fetters, *Polymer*, 1987, **28**, 1997–2003.
32 W. W. Graessley, *Polymeric liquids & networks: Structure and properties*, Garland Science, New York, 2004.
33 K.-G. Wahlund, in *Field-flow fractionation handbook*, ed. M. Schimpf, K. Caldwell and J. C. Giddings, Wiley, New York, 2000, pp. 279–294.